



Practical use of the regression offset approach for the prediction of *in vivo* intrinsic clearance from hepatocytes

Anna-Karin Sohlenius-Sternbeck, Christopher Jones, Douglas Ferguson, Brian J. Middleton, Denis Projean, Eva Floby, Johan Bylund & Lovisa Afzelius

To cite this article: Anna-Karin Sohlenius-Sternbeck, Christopher Jones, Douglas Ferguson, Brian J. Middleton, Denis Projean, Eva Floby, Johan Bylund & Lovisa Afzelius (2012) Practical use of the regression offset approach for the prediction of *in vivo* intrinsic clearance from hepatocytes, *Xenobiotica*, 42:9, 841-853, DOI: [10.3109/00498254.2012.669080](https://doi.org/10.3109/00498254.2012.669080)

To link to this article: <https://doi.org/10.3109/00498254.2012.669080>



Published online: 18 Apr 2012.



Submit your article to this journal [↗](#)



Article views: 1778



View related articles [↗](#)



Citing articles: 13 View citing articles [↗](#)

RESEARCH ARTICLE

Practical use of the regression offset approach for the prediction of *in vivo* intrinsic clearance from hepatocytes

Anna-Karin Sohlenius-Sternbeck¹, Christopher Jones², Douglas Ferguson³, Brian J. Middleton⁴, Denis Projean⁵, Eva Floby¹, Johan Bylund^{1,6}, and Lovisa Afzelius⁷

¹DMPK, CNSP iMed, AstraZeneca R&D Södertälje, Sweden, ²DMPK, Oncology iMed, AstraZeneca R&D Alderley Park, Macclesfield, Cheshire, UK, ³DMPK, Infection iMed, AstraZeneca R&D Boston, Waltham, MA 02451, USA, ⁴Discovery Statistics, Discovery Sciences, AstraZeneca R&D Alderley Park, Macclesfield, Cheshire, UK, ⁵DMPK Centre of Excellence, AstraZeneca R&D Montreal, Saint-Laurent, Quebec, Canada, ⁶Pharmaceutical Biosciences, Uppsala Biomedical Centre, Uppsala University, Uppsala, Sweden, and ⁷Project Management, CNSP iMed, AstraZeneca R&D Södertälje, Sweden

Abstract

1. Systematic under-prediction of clearance is frequently associated with *in vitro* kinetic data when extrapolated using physiological scaling factors, appropriate binding parameters and the well-stirred model. The present study describes a method of removing this systematic bias through application of empirical correction factors derived from regression analyses applied to the *in vitro* and *in vivo* data for a defined set of reference compounds.
2. Linear regression lines were established with *in vivo* intrinsic clearance (CL_{int}), derived from *in vivo* clearance data and scaled *in vitro* intrinsic clearance from isolated hepatocyte incubations. The scaled CL_{int} was empirically corrected to a predicted *in vivo* CL_{int} using the slope and intercept from a uniform weighted linear regression applied to the *in vitro* to *in vivo* extrapolation.
3. Cross validation of human data demonstrated that 66% of the reference compounds had a predicted *in vivo* CL_{int} within two-fold of the observed value. The average absolute fold error (AAFE) for the *in vivo* CL_{int} predictions was 1.90. For rat, 54% of the compounds had a predicted value within two-fold of the observed and the AAFE was 1.98.
4. Three AstraZeneca projects are used to exemplify how a two-sided prediction interval, applied to the rat regression corrected reference data, can form the basis for assessing the likelihood that, for a given chemical series, the *in vitro* kinetic data is predictive of *in vivo* clearance and is therefore appropriate to guide optimisation of compound metabolic stability.

Keywords: Liver, metabolism, hepatocytes, CL_{int}, *in vitro* to *in vivo* scaling, regression offset, well-stirred model

Introduction

The routine determination of *in vitro* intrinsic clearance (CL_{int}) in drug discovery is well established within the pharmaceutical industry (Grime & Riley 2006). The utility of these *in vitro* CL_{int} assays for rank ordering of compounds based on their intrinsic metabolic stability; evaluating chemical structure property relationships to aid compound design and for extrapolation to predictions of metabolic clearance in pre-clinical species and humans has been widely demonstrated (Houston 1994; McGinnity et al. 2004; Hallifax et al. 2008). Isolated hepatocytes

provide an intact cellular system containing a full complement of drug metabolising enzymes, transporters and cofactors, making them ideal for studying rates of drug metabolism (Brandon et al. 2003; Donato & Castell 2003; Hewitt et al. 2007). Over the last 5–10 years, the use of human hepatocytes in metabolism-based assays has increased substantially. In part, this can be attributed to developments in cryopreservation procedures facilitating routine access to high quality cryopreserved human hepatocytes. A number of studies have demonstrated

Address for Correspondence: Anna-Karin Sohlenius-Sternbeck, DMPK, CNSP iMed, AstraZeneca R&D Södertälje, SE-151 85 Södertälje, Sweden. E-mail: anna-karin.sternbeck@astrazeneca.com

(Received 21 December 2011; revised 17 February 2012; accepted 20 February 2012)

rates of metabolism in cryopreserved and fresh hepatocytes to be comparable (Li et al. 1999; Naritomi et al. 2003; McGinnity et al. 2004; Floby et al. 2009).

Extrapolation of microsome- or hepatocyte-derived intrinsic clearances commonly results in an underestimation of the *in vivo* value, despite incorporation of established physiological scaling factors (SFs) and the unbound fractions in both blood and *in vitro* matrix (Obach 1999; Ito & Houston 2004; Brown et al. 2007; Riley et al. 2005; Stringer et al. 2008). There are a number of plausible explanations for this observation. For example, it is known that the *in vitro* incubation conditions employed can greatly influence the rate of drug metabolism (Grime & Riley 2006). This observed under-prediction is a major challenge that researchers, industrywide, are facing. Previous authors have described scaling approaches in which empirical, or drug specific, SFs have been successfully applied to correct for under-predictions observed across a range of drugs (Ito & Houston 2005; Riley et al. 2005; Grime & Riley 2006; Stringer et al. 2008; Hallifax et al. 2010; Sohlenius-Sternbeck et al. 2010).

In this work the practical application of the regression offset approach for prediction of *in vivo* CLint is discussed (Riley et al. 2005; Ito & Houston 2005; Grime & Riley 2006; Sohlenius-Sternbeck et al. 2010). The principles of this approach are described in detail and also how it is applied within AstraZeneca's research programmes.

Human and rat linear regression equations were established using data generated on reference compounds (Tables 1 and 2, respectively). Reference compounds were selected on the basis of having hepatic metabolic clearance as the principal route of elimination. Additionally, known substrates for hepatic uptake transporters were avoided in case metabolism was not the rate-limiting step in the elimination process (Soars et al. 2009). The reference compounds showed chemical diversity representative of AZ chemical space, based on their physicochemical properties. The regression equations were used to empirically correct the scaled CLint to a predicted *in vivo* CLint (see Table 3, for CLint nomenclature). The derived *in vivo* CLint was then plotted on the *Y* axis against the predicted *in vivo* CLint on the *X* axis to visualise the *in vitro* to *in vivo* extrapolation (IVIVE). For the rat (or other preclinical species), project data can be overlaid on the same graph as the reference compound data used to generate the regression offset equation. To evaluate the overall performance of the IVIVE, which encompassed the *in vitro* assay and the scaling approach, cross validation was used (see 'Materials and methods' section).

Previously, as a means to judge whether a compound 'scales', arbitrary cut-off values (e.g. within three-fold of the observed) have been proposed based on the unbound *in vivo* CLint (Houston & Carlile 1997). A novel aspect to the approach described in this paper relates to application of a two-sided prediction interval (powered at 80%) to the regression corrected reference data. This is a way of visualising IVIVE in drug discovery projects and it provides a basis to impartially assess the likelihood

that a derived *in vivo* CLint (or blood clearance) for a prospective compound or chemical series is predictable from *in vitro* kinetic data. Accurate IVIVE in rat enables *in vitro* CLint data to be used to develop chemical structure property relationships relating to metabolic stability and clearance for efficient compound design. It also builds confidence that the same scaling approach can be used for projection of human hepatic metabolic clearance. Taking three active and chemically diverse AstraZeneca projects as examples, we show how this clearance prediction approach is used in practice. To the best of the authors' knowledge, this is the first time that non-arbitrary criteria have been proposed for making such assessments.

Materials and methods

All reference compounds were obtained from the AstraZeneca compound collection. AstraZeneca compounds were synthesised at AstraZeneca R&D Södertälje (Södertälje, Sweden). All other chemicals were of analytical grade and obtained from commercial suppliers.

In vitro experiments

Cryopreserved human hepatocytes were obtained from CellzDirect Inc (www.cellzdirect.com) (Durham, NC, USA). The experiments were performed, as described previously (Sohlenius-Sternbeck et al. 2010), with pooled hepatocytes constituted from five individual donors that were combined post thawing to give a representation of an average human donor pool. This was achieved by using the vendor's donor characterisation data (enzyme activity) from all available donors to calculate a mean activity of phase I and phase II enzymes (i.e. 7-ethoxycoumarin-O-deethylation, 7-hydroxycoumarin glucuronidation, 7-hydroxycoumarin sulphatation and cytochrome P4501A2, 2C9, 2C19, 2D6 and 3A4), which was considered as an 'average donor'. Donors (male and females) were then selected so that the average enzyme activity of the pool should resemble this 'average donor'.

Fresh hepatocytes were isolated from male Sprague-Dawley rats, as described previously (Floby et al. 2004), using a collagenase perfusion technique, modified from the procedure described by Bissell and Guzelian (1980).

Hepatocyte viabilities (as determined by Trypan blue exclusion) were routinely 80–90%. All hepatocyte incubations were performed in 96-well deep microplates (Treff Ag, Degersheim, Switzerland). The assay setup was somewhat different from the assay setup described previously (Sohlenius-Sternbeck et al. 2010). In the present study, the incubation volume was lower, and the *in vitro* reaction was stopped with a higher proportion of acetonitrile. The hepatocytes were diluted in Williams medium E and 45 µL of the cell suspension was added to 5 µL of a 10 µM solution of each compound so that the final hepatocyte concentration was 1×10^6 cells/mL, and the concentration of compound was 1 µM. Each experiment was, in general, repeated at least twice. On each occasion, the incubations were repeated in duplicate at

Table 1. Reference compounds used for the building of a human regression line.

Drug name	Ion class	f_u^*	R_b	LogP/D ^o	Observed plasma clearance (mL/min/kg)	Blood clearance calculated from plasma clearance (mL/min/kg)	<i>In vitro</i> raw CL _{int} (μL/min/10 ⁶ cells)	Predicted <i>in vivo</i> CL _{int} [‡] (mL/min/kg)
Acetaminophen	N	0.89	1.00 ^e	0.29	4 ^b	4	1.3	9.5
Bufuralol	B	0.176 [§]	0.80 ^d	3.267 [#]	8.9 ^a	11	15.8	24.3
Caffeine	N	0.742	1.08 ^d	-0.06	1.4 ^a	1.3	1.2	9
Carvedilol	B	0.009	0.70 ^g	4.314	7.8 ^a	11	44	11.4
Chlorpromazine	B	0.016	0.78 ^{d,i}	5.433	8.6 ^b	11	18.1	31.6
Clozapine	B	0.047	0.87 ^j	3.627	2.5 ^a	2.9	7.7	7.1
Desipramine	B	0.16	0.96 ^{d,i}	4.001	11 ^a	11	3.9	11.3
Diazepam	N	0.013	0.78 ^{i,e,g}	2.81	0.38 ^a	0.49	1.2	0.9
Diclofenac	A	0.002 [§]	0.55 ⁱ	1.12	3.5 ^a	6.4	32.7	2
Diflunisal	A	0.001 [§]	0.55	0.26	0.1 ^b	0.2	2.1	0.2
Diltiazem	B	0.25	0.98 ^{e,k}	2.793	13 ^a	13	7.4	15.1
Etodolac	A	0.008	0.60 ^g	0.5	0.72 ^b	1.2	7.9	1.9
Fenoprofen	A	0.002 [§]	0.55	0.58	0.93 ^b	1.7	7.2	0.8
Gemfibrozil	A	0.002 [§]	0.55	1.94	1.7 ^b	3.1	30.7	2.7
Glipizide	A	0.014 [§]	0.55	0.4	0.56 ^b	1	0.9	0.7
Granisetron	B	0.722 [§]	1	2.368	9.1 ^a	9.1	2.5	13.1
Ibuprofen	A	0.003 [§]	0.55 ⁱ	0.88	0.75 ^b	1.4	8	1.1
Imipramine	B	0.125	1.07 ^{c,i}	4.633	9.46 ^b	8.8	7.3	20.3
Irbesartan	Z	0.023 [§]	0.55	1.3	2.3 ^a	4.2	14.3	6.4
Ketoprofen	A	0.004 [§]	0.55	-0.145	0.91 ^b	1.7	2.3	0.6
Methyl-Prednisolone	N	0.26	1	2.12	7.5 ^b	7.5	1.9	5.8
Metoprolol	B	0.883 ^a	1.07 ^{d,g}	1.753	13 ^a	12	6.2	26.8
Midazolam	N	0.023	0.67 ^{g,i}	3.4	5.3 ^a	8	16	7.2
Naloxone	B	0.722 [§]	1.22 ^c	2.283	19.6 ⁿ	16.1	37.9	76.1
Omeprazole	N	0.18	0.60 ^{e,g}	2.115	8.4 ^a	14	3.8	9.6
Ondansetron	B	0.353 [§]	0.83 ^g	2.162	5.8 ^a	7	1.8	7.7
Oxaprozin	A	0.001 [§]	0.55	1.15	0.039 ^b	0.071	1.6	0.1
Oxazepam	N	0.033	1.11 ^d	2.560 [#]	1.1 ^a	1	3.3	1.9
Pindolol	B	0.84	0.69 ^g	1.859	4.2 ^b	6.1	2.1	17
Prazosin	N	0.038	0.70 ^g	2.02	2.7 ^b	3.9	4.9	3.8
Prednisolone	N	0.483 [§]	1	1.6	2.9 ^a	2.9	1.7	8
Propranolol	B	0.205	0.86 ^{c,d}	3.421	12:00 AM	14	19.9	33
Quinidine	B	0.18	0.90 ^{d,i}	3.547	4:00 AM	4.5	3.2	9.1
Ranitidine	B	0.496 [§]	1	-0.096	3.2 ^b	3.2	1.4	7.9
Ritonavir	N	0.021 [§]	0.59 ^k	4.25	1.2 ^b	2	3.2	10.6
Sildenafil	B	0.066 [§]	0.63 ^k	2.8	6 ^b	10	13.4	10.8
Theophylline	N	0.456 ^{a,b,d}	0.83 ^d	-0.115	0.533 ^m	0.642	1	6.9
Timolol	B	0.77	0.84 ^c	1.783	7.8 ^a	9.3	2.8	17.3
Tolbutamide	A	0.021	0.68 ^{d,k}	0.395	0.24 ^a	0.4	0.7	0.6
Verapamil	B	0.129	0.77 ⁱ	3.961	11.8 ^b	15.3	23.1	34.9
Zolpidem	N	0.061	0.76 ⁱ	2.020 [#]	4.3 ^a	5.7	3.3	4.4

The human clearance values have been adjusted, where the renal clearance was known.

f_u = fraction unbound in plasma;

R_b = blood-to-plasma ratio;

N = neutral; B = base; A = acid; Z = zwitterions;

* Measured at AstraZeneca in Södertälje (see Methods and Materials) unless other is indicated;

§ Value obtained from AstraZeneca in Alderley Park;

Value predicted in silico using AstraZeneca QSAR models;

^o Calculated logP for bases, measured logD for other ion classes;

[‡] Obtained after cross validation (for further details see 'Methods' section);

^a Obach et al. (2008);

^b Riley et al. (2005);

^c Shibata, et al. (2002);

^d Brown, et al. (2007);

^e Naritomi, et al. (2003);

^f Lave, et al. (1997);

^g Paixao, et al. (2009);

^h Paine, et al. (2008);

ⁱ Obach (1999);

^j Loi, et al. (1999);

^k Value quoted in simCYP software;

^l Youdim, et al. (2008);

^m Goodman, et al. (1996);

ⁿ McGinnity, et al. (2004).

Table 2. Reference and in-house compounds used to build the rat regression line.

Drug name	Ion class	f_{up}^*	R_b	LogP/D ^o	Observed plasma clearance (mL/min/kg)	Blood clearance calculated from plasma clearance (mL/min/kg)	<i>In vitro</i> raw CLint (μ L/min/ 10^6 cells)	Predicted <i>in vivo</i> CLint [‡] (mL/min/kg)
Diclofenac	A	0.009	0.55	1.24	9.9	18	27.7	21.6
Granisetron	B	0.61	1	2.7	41	41	54.9	509
Midazolam	N	0.053	1	3.92	31.9	31.9	23	57.8
Pindolol	B	0.64	1	1.55	59	59	47.4	323
Prazosin	N	0.33	1	1.56	30	30	8.1	59.7
Ritonavir	N	0.043	1	5.1	30	30	10	85.4
AZ1	A	0.014	0.55	2.61	6.2	11.3	11.6	17.6
AZ2	A	0.039	0.55	2.4	8.7	15.8	20.1	46.8
AZ3	A	0.019	0.55	2.05	6.5	11.8	6.6	13.5
AZ4	B	0.032	1	3.2	36.3	36.3	20.3	30.4
AZ5	B	0.162	1	3.23	56.6	56.6	24.2	90.8
AZ6	B	0.016	1	3.45	9.3	9.3	29.1	28.5
AZ7	B	0.038	1	3.53	13.3	13.3	4.1	13.1
AZ8	B	0.136	1	1.89	57.3	57.3	29.9	98.1
AZ9	N	0.05	1	3.03	45.9	45.9	28.2	49.8
AZ10	N	0.029	1	5.56	23.2	23.2	12	127
AZ11	N	0.086	1	2.65	40	40	5	20
AZ12	N	0.086	1	3.14	50.1	50.1	14	41.9
AZ13	N	0.076	1	2.94	33	33	3.6	15
AZ14	N	0.036	1	3.18	21.4	21.4	6.9	15.4
AZ15	N	0.089	1	2.42	32	32	14.1	40.8
AZ16	N	0.03	1	3.1	17.3	17.3	7.5	16
AZ17	N	0.186	1	2.07	13.1	13.1	3.3	24.8
AZ18	N	0.085	1	2.93	47.4	47.4	16.7	47.2
AZ19	B	0.09	1	1.75	53.1	53.1	36.7	73.1
AZ20	B	0.013	1	4.02	38.7	38.7	23	23.5
AZ21	B	0.101	1	2.28	40.8	40.8	41	91.4
AZ22	B	0.011	1	4.25	17.7	17.7	37	34.4
AZ23	A	0.002	0.55	3.55	4.8	8.8	17	7.4
AZ24	N	0.062	1	3.57	7.9	7.9	5	21.2
AZ25	N	0.127	1	1.9	17.1	17.1	4.6	23.8
AZ26	N	0.036	1	2.43	7.3	7.3	5.9	13.2
AZ27	B	0.017	1	3.82	19.3	19.3	41.2	40.2
AZ28	B	0.084	1	2.83	17	17	9.7	30.8
AZ29	B	0.045	1	3.73	22.1	22.1	23.3	52
AZ30	N	0.056	1	3.86	50.2	50.2	50.5	113
AZ31	N	0.062	1	2.85	55.7	55.7	25.9	50.4
AZ32	N	0.064	1	2.82	24.8	24.8	10.4	28.8
AZ33	N	0.133	1	2.89	51.3	51.3	21	71.9
AZ34	N	0.076	1	3.54	32.4	32.4	11.7	38.3
AZ35	A	0.001	0.55	3.98	0.8	1.5	2.8	1.7
AZ36	N	0.083	1	3.59	16.2	16.2	8.8	37.6
AZ37	A	0.001	0.55	4.01	1.1	2	12.5	4.7
AZ38	N	0.19	1	3.06	39.9	39.9	31.9	124
AZ39	N	0.047	1	3.47	41.6	41.6	29.9	50.3
AZ40	B	0.14	1	2.07	13.3	13.3	8.9	39.4
AZ41	B	0.14	1	1.9	8.7	8.7	7.3	38.3
AZ42	B	0.16	1	2.07	39.9	39.9	12.7	59.4
AZ43	B	0.022	1	2.47	13.7	13.7	14.1	17.1
AZ44	B	0.11	1	3.15	18.9	18.9	16.7	57.8
AZ45	N	0.28	1	3.59	24.6	24.6	14.1	126
AZ46	A	0.001	0.55	4.06	1.2	2.2	13.5	4.8

(Continued)

Table 2. (Continued).

Drug name	Ion class	$f_{u_p}^*$	R_b	LogP/D ^a	Observed plasma clearance (mL/min/kg)	Blood clearance calculated from plasma clearance (mL/min/kg)	<i>In vitro</i> raw CL _{int} (μL/min/10 ⁶ cells)	Predicted <i>in vivo</i> CL _{int} [‡] (mL/min/kg)
AZ47	N	0.009	1	3.54	3.6	3.6	10.4	9.8
AZ48	N	0.29	1	2.92	33.1	33.1	23.2	160
AZ49	B	0.008	1	2.63	4.4	4.4	26.8	13.8
AZ50	B	0.011	1	2.55	15.3	15.3	48.1	22.9

The rat clearance values have been adjusted, where the renal clearance was known.

f_{u_p} = fraction unbound in plasma;

R_b = blood-to-plasma ratio (estimated);

N = neutral; B = base; A = acid; Z = zwitterions;

* Measured at AstraZeneca in Södertälje (see 'Methods and materials');

^a cLogP for bases, ACD logD for other ion classes;

[‡] Obtained after cross validation (for further details, see 'Methods' section).

Table 3. Definitions of clearance.

Concept	Definition
<i>In vitro</i> raw CL _{int}	Intrinsic clearance that is directly derived from the first-order rate constant describing the decline in compound concentration in isolated hepatocytes incubations. No correction for incubational binding has been applied.
Scaled CL _{int}	An intrinsic clearance scaled to the liver using the <i>in vitro</i> raw CL _{int} , physiological SFs and the fractions unbound in blood and the <i>in vitro</i> incubation.
Predicted <i>in vivo</i> CL _{int}	The predicted intrinsic clearance of the liver obtained after regression correcting the scaled CL _{int} . (Note: This is the CL _{int} as viewed from total blood concentration rather than free blood concentration.)
Predicted <i>in vivo</i> clearance	<i>In vivo</i> clearance predicted by application of the WSM to the 'Predicted <i>in vivo</i> CL _{int} '.
Observed plasma clearance	The <i>in vivo</i> clearance observed from plasma.
Observed blood clearance	The <i>in vivo</i> clearance observed from blood. Obtained either from the observed plasma clearance by dividing by the blood-to-plasma ratio or by direct measurement of blood PK samples.
Derived <i>in vivo</i> CL _{int}	The total <i>in vivo</i> intrinsic clearance of the liver as viewed from total blood concentration. This is derived from application of the well-stirred-model to the 'observed blood clearance'.

37°C under an atmosphere of 5% CO₂/95% air and the plates were shaken gently. The human hepatocytes were incubated with compound for 0, 15, 30, 60 and 90 min, while the rat hepatocytes were incubated for 0, 5, 15, 30 and 60 min. The reactions were stopped by the addition of 150 μL ice-cold acetonitrile. The plates were centrifuged (1900 × *g* for 5 min) and aliquots of the supernatant analysed by LC-MS/MS (Sohlenius-Sternbeck et al. 2010).

As a quality control measure, to confirm the reproducibility of the CL_{int} assay over time, each experiment included an incubation containing a cocktail of probe substrates, incubated under comparable experimental conditions (2 μM of phenacetin, diclofenac, diazepam, bufuralol, midazolam and 7-hydroxycoumarin).

Those test compounds with a human CL_{int} value below the statistical limit of quantification (see below) in the standard assay, were re-incubated and more time points were sampled (0.5, 15, 30, 45, 60, 75 and 120) to increase the precision of the CL_{int} measurement. The CL_{int} values were obtained from disappearance curves where the substrate concentration was plotted against the time. The concentration of each reference compound in the hepatocyte incubation was fitted to a first-order elimination equation:

$$C = C_0 \cdot e^{-k \times t} \quad (1)$$

where *C* is the measured concentration at any time, *C*₀ is the concentration at zero-time and *k* is the elimination constant. The decrease in substrate was exponential over time for all reported CL_{int} values. Curve fit was performed after natural logarithm transformation of the concentration data. Therefore, data could be fit to Equation (1) by linear regression and data was considered to fit the equation well when the *p*-value was <0.05. For most compounds the *p*-value was <0.01. Stable compounds with *p* > 0.05 (generally with CL_{int} < 1 μL/min/10⁶ cells) were not included in this work.

Intrinsic clearance was calculated as follows:

$$CL_{int} = k \cdot V \quad (2)$$

where *V* is the volume of the hepatocyte suspension.

The calculations were performed by employing a Microsoft® Excel 2000-based standardised protocol and XLFit (version 2.1.2, Guildford, UK). All regressions were evaluated by correlation coefficients and *p* values for type I errors.

Plasma protein binding

Plasma protein binding was determined by equilibrium dialysis method (Sohlenius-Sternbeck et al. 2010) and measurements of logD and pK_a were performed, according to Wenlock et al. (2011).

Rat pharmacokinetic studies

Rat pharmacokinetic studies were performed, according to the method described by Briem et al. (2007), to enable calculation of the derived *in vivo* CL_{int}.

Fraction unbound in incubation

The fraction unbound in the hepatocyte incubation (fu_{inc}) was predicted, according to Kilford et al. (2008):

$$fu_{inc} = \frac{1}{1 + 125 \times V_R \times 10^{0.072 \times \log P / D^2} + 0.067 \times \log P / D - 1.126} \quad (3)$$

where V_R is the ratio between the cell volume and the incubation volume and it has a value of 0.005 at a cell concentration of 10^6 cells/mL. For human fu_{inc} predictions, measured logD (Wenlock et al. 2011) and calculated logP were used. The Henderson–Hasselbalch relationship was used for calculation of logP for basic compounds from measured logD and pKa accordingly:

$$\log P = \log D + \log[1 + 10^{pKa - 7.4}] \quad (4)$$

For rat fu_{inc} , an in-house QSAR model of logP (clogP) was built from AstraZeneca's internal datasets and physicochemical descriptors. ACD/logD (version 12.0) is a commercial package from Advanced Chemistry Development (Toronto, Canada) that was used to predict logD.

Building the regression line using reference compounds

A schematic showing the steps taken to transform the *in vitro* raw CL_{int} to a predicted *in vivo* clearance using the regression approach is shown in Figure 1. The *in vitro* raw CL_{int} values for the model reference compounds are scaled to a liver CL_{int} according to

$$\text{Scaled CL}_{int} = \frac{CL_{int} \times SF \times fu_b}{fu_{inc}} \quad (5)$$

The physiological SFs were $(120 \times 10^6 \text{ cells/g liver}) \times (1680 \text{ g liver/70 kg body weight})$ for human hepatocytes and $(163 \times 10^6 \text{ cells/g liver}) \times (10 \text{ g liver/0.25 kg body weight})$ for rat hepatocytes. The rat hepatocellularity value was

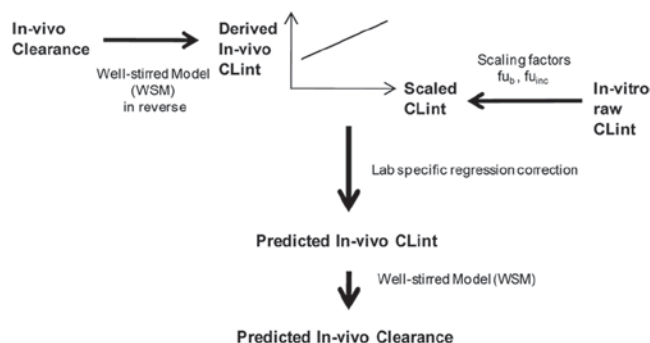


Figure 1. Prediction of metabolic clearance. Reference compounds were used to establish the regression offset equation, which was subsequently used for the prediction of *in vivo* CL_{int} and clearance for any project compound.

determined by Smith et al. (2008), while the human hepatocellularity number lies within the 95% confidence interval referenced from the extensive analysis by Barter et al. (2007).

The blood-to-plasma ratio, R_b , was used to calculate the *in vivo* blood clearance (CL_b) from the *in vivo* plasma clearance (CL_p):

$$CL_b = \frac{CL_p}{R_b} \quad (6)$$

The fraction unbound in the blood (fu_b) was estimated as follows:

$$fu_b = \frac{fu_p}{R_b} \quad (7)$$

where fu_p is the fraction unbound in plasma. When no measured R_b value was available, a default value of 0.55 (1-haematocrit) was assumed for acidic compounds and 1 for other ion classes. This approach has also been used by others (Riley et al. 2005; Hallifax et al. 2010).

The *in vivo* CL_{int} (as viewed from total blood concentration) was derived from the observed *in vivo* CL_b for the reference compounds using the rearranged well-stirred model (WSM):

$$\text{Derived in vivo CL}_{int} = \frac{CL_b \times Q_h}{Q_h - CL_b} \quad (8)$$

Hepatic blood flow (Q_h) was taken as 20 and 72 mL/min/kg for human and rat, respectively (Brown et al. 1997; Delp et al. 1998).

To establish the regression line, log [derived *in vivo* CL_{int}] on the Y axis was plotted against log[CL_{int} × SF × fu_b/fu_{inc}] on the X axis. All measured and predicted *in vitro* variables (including fu_b) are therefore grouped together on the X axis. This is somewhat different from the traditional approach, where unbound CL_{int} has been correlated with CL_{int} *in vivo* corrected with fu_b . The reason for grouping the data as described here is that it facilitates analysis of error-propagation in projection of human clearance and the likely uncertainty associated with these predictions (this is an area of interest currently being investigated). The regression offset equation is shown below:

$$\text{Log} \left[\left(\frac{CL \times Q_h}{Q_h - CL} \right) \right] = b \times \text{log} \left[CL_{int} \times SF \times \left(\frac{fu_b}{fu_{inc}} \right) \right] + a \quad (9)$$

where a is the intercept and b the slope.

Application of the regression line for predictions of *in vivo* CL_{int}

The *in vitro* raw CL_{int} value is converted to a scaled CL_{int}, according to Equation (5). The slope and intercept from the regression offset equation are then used to calculate the log predicted *in vivo* CL_{int}, that is, $\log[(CL_b \times Q_h)/$

$(Q_h - CL_h)$. The predicted blood clearance is calculated by using the WSM:

$$\text{Predicted blood } CL_h = \frac{Q_h \times \text{predicted } in \text{ vivo } CL_{int}}{Q_h + \text{predicted } in \text{ vivo } CL_{int}} \quad (10)$$

Regression corrected IVIVE

The regression corrected IVIVE plot is the log derived *in vivo* CL_{int} from Equation (8) plotted against the log predicted *in vivo* CL_{int} from Equation (9).

Statistics

Cross validation to assess model performance for IVIVE

The compounds in the rat regression line were randomly divided into six groups, with 9 or 10 compounds per test group. One group (test group) was removed from the total data set and the remaining compounds (model group) were used for linear regression analysis. The intercept and slope derived from the regression were in turn used to generate the predicted *in vivo* CL_{int} values for the compounds in the test group that had been removed. This process was repeated for all six groups providing unbiased error rates for the *in vivo* CL_{int} predictions and avoiding the same data being used to generate and test the regression model.

The cross validation of human data was performed, as described above, with the compounds randomly divided into six groups, with 6 or 7 compounds per test group.

Performance evaluation

From the regression corrected IVIVE plot, a measure of the bias, expressed as the average fold error (AFE), that is, the geometric mean fold error, was calculated as follows (Tang et al. 2007):

$$AFE = 10^{\frac{1}{N} \sum \log \left(\frac{\text{observed}}{\text{predicted}} \right)} \quad (11)$$

The average absolute fold error (AAFE), a measure of the precision, was calculated using the following equation (Tang et al. 2007):

$$AAFE = 10^{\frac{1}{N} \sum \left| \log \left(\frac{\text{observed}}{\text{predicted}} \right) \right|} \quad (12)$$

Prediction limits

These are the appropriate limits when predicting *in vivo* CL_{int} for future compounds outside the dataset defining the regression (Armitage & Berry 1994). They incorporate the variability about the regression with the uncertainty in the regression line itself. The prediction limits were calculated as follows:

$$\begin{aligned} \text{Log}_{10}(Y) = & \text{Intercept} + \text{slope} * \text{Log}_{10}(X) \\ & + s * t * \sqrt{1 + \frac{1}{N} + \frac{(X - \bar{X})^2}{\text{Exx}}} \end{aligned} \quad (13)$$

where Y is the derived *in vivo* CL_{int}, X is the scaled CL_{int}, s , t , N , \bar{X} , Exx are all based on the regression data collected.

s = standard deviation (SD) about regression line;
 t = critical Student t -value with $N-2$ degrees of freedom (df);
 N = number of observations forming the regression;
 \bar{X} = mean of $\log_{10}(\text{scaled CL}_{int})$;
 Exx = corrected sum of squares of $\log_{10}(\text{scaled CL}_{int})$.

Results

Quality control CL_{int} data

The mean and standard deviation (SD) associated with the quality control CL_{int} data have been presented in Table 4. The data was generated over a period of 6 months during which time the data for the regression line and project compounds was completed. Figure 2 shows an example quality control (QC) monitoring plot for bufuralol CL_{int} in rat hepatocytes. No change was observed in the QC monitoring line demonstrating that the CL_{int} assay was reproducible and comparable over this period.

Human *in vivo* CL_{int} predictions

The reference compounds used to derive the human linear regression line are shown in Table 1. This table also provides information on ion class, f_u , and R_b values, calculated $\log P$ or measured $\log D$, observed plasma

Table 4. CL_{int} values for cocktail substrates used for quality control of CL_{int} experiments. The cocktail was incubated with suspensions of freshly isolated rat hepatocytes and cryopreserved human hepatocytes.

Substrate	CL _{int} (μL/min/10 ⁶ cells)	
	Rat	Human
7-Hydroxycoumarin	73.0 ± 11.4	45.0 ± 5.0
Diclofenac	30.9 ± 6.9	44.9 ± 5.0
Midazolam	36.8 ± 5.6	23.2 ± 2.7
Phenacetin	20.7 ± 1.4	24.3 ± 3.5
Bufuralol	69.2 ± 6.8	15.5 ± 2.2
Diazepam	21.0 ± 4.3	1.5 ± 0.3

Data is mean ± standard deviation of eight experiments.

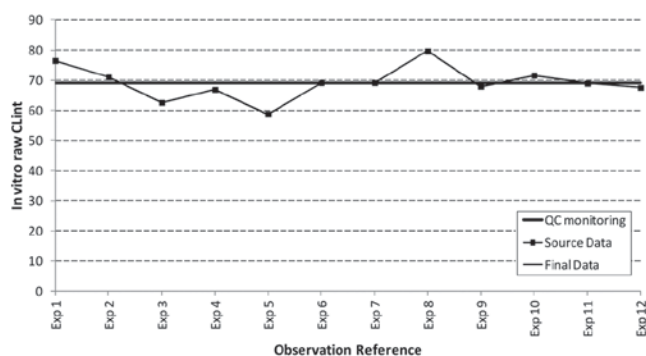


Figure 2. QC monitoring plot for bufuralol rat hepatocyte CL_{int}. Individual occasion (mean) CL_{int}s were plotted against occasion and a cusum (Woodward & Goldsmith 1964) used to assess if there has been any step changes over time in the assay indicated by the solid black line.

clearance, calculated observed blood clearance, *in vitro* raw CLint and predicted *in vivo* CLint. Any known renal clearance has been subtracted from the total clearance.

Figure 3A shows the human hepatocyte regression line established with unbound CLint correlated with *in vivo* CLint corrected with $f_{u,b}$ (i.e. the traditional approach to show an *in vitro* to *in vivo* correlation). In this case, the correlation, R^2 , was 0.60. Cross validation of human data demonstrated that 48% of the compounds had a predicted unbound *in vivo* CLint within two-fold of the derived unbound *in vivo* CLint and the AAFE for the predictions were 2.6 (data not shown).

However, when all measured and predicted *in vitro* variables are grouped together on the X axis, the R^2 between log-scaled CLint and log-derived *in vivo* CLint was 0.77 (Figure 3B), and the relationship was described by

$$Y = 0.660x + 0.633$$

Cross validation of human data demonstrated that 66% of the compounds had a predicted *in vivo* CLint within two-fold of the derived *in vivo* CLint and the AAFE for the predictions were 1.90, while for non-regression corrected

data, only 32% where within two-fold and the AAFE was 4.2 (Table 5).

In Figure 3C, the regression corrected *in vitro* to *in vivo* correlation is shown (with the slope now equal to 1).

When estimated blood-to-plasma ratios were used instead of measured values, for those compounds where a measured value existed ($n=30$), the R^2 between log-scaled CLint and log-derived *in vivo* CLint was 0.74 (graph not shown), and cross validation demonstrated that 68% of the compounds had a predicted *in vivo* CLint within two-fold of the derived *in vivo* CLint and the AAFE for the predictions were 2.0 (Table 5).

Rat *in vivo* CLint predictions

Table 2 shows information about the reference and in-house compounds used for the rat regression analysis together with information on ion class, $f_{u,p}$, predicted logD (ACD logD) or estimated logP (clogP), observed plasma clearance, calculated observed blood clearance, *in vitro* raw CLint and predicted *in vivo* CLint. Ion class-specific default values were used for R_b (rather than measured values) to establish the predictive accuracy of the IVIVE method based upon the minimal *in vitro*

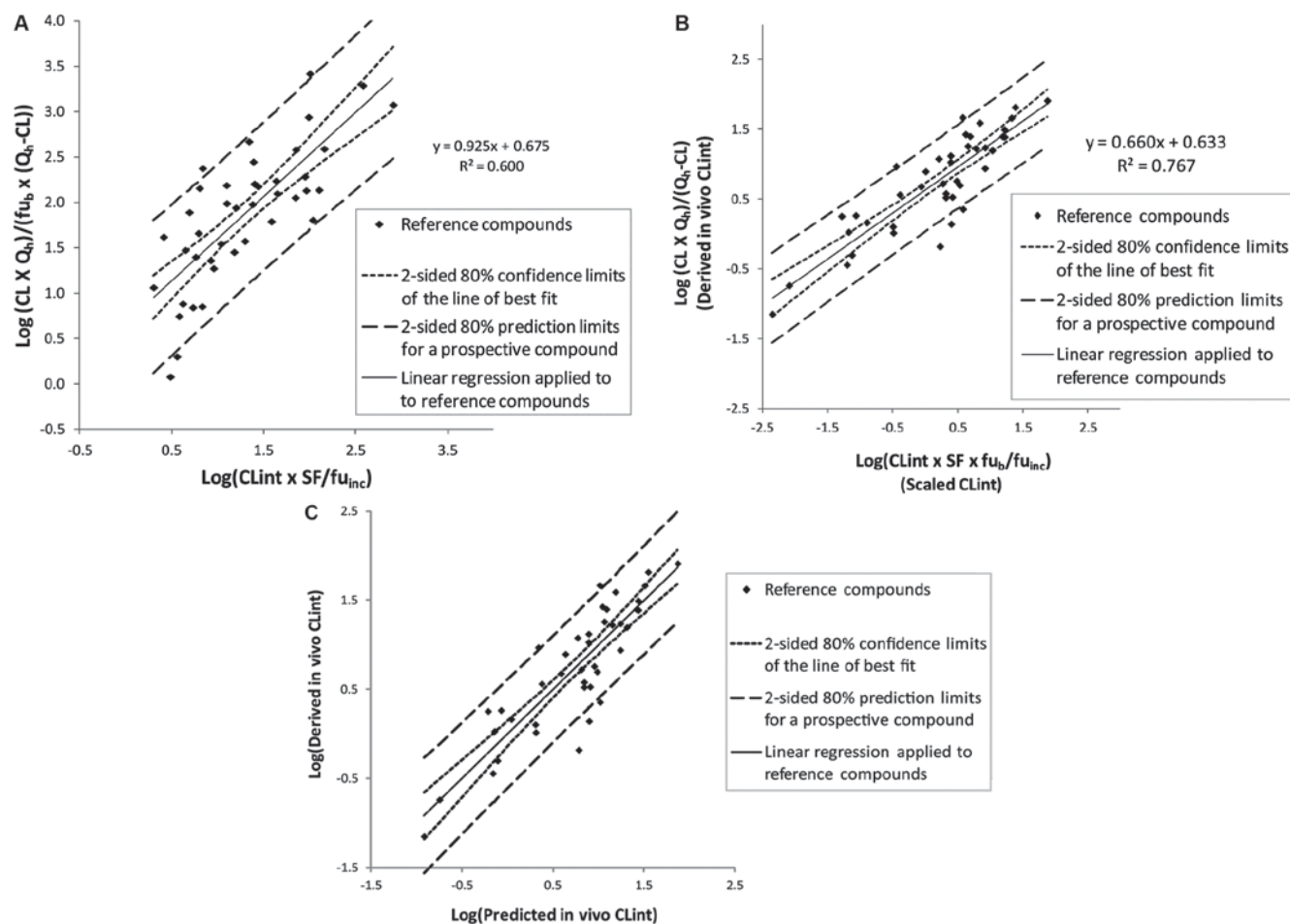


Figure 3. (A–C) The human hepatocyte regression line (A) traditionally established with unbound CLint correlated with CLint *in vivo* corrected with $f_{u,b}$; (B) with all measured and predicted *in vitro* variables grouped together on the X-axis and (C) the corresponding regression corrected IVIVE plot.

data (hepatocyte CL_{int} and f_{up}) that would routinely be available in early compound screening. The correlation, R^2 , between log-scaled CL_{int} and log-derived *in vivo* CL_{int} was 0.62 (Figure 4A) and the relationship was described by

$$Y = 0.662x + 0.974$$

Statistical analysis of the cross validated rat data demonstrated that 54% of the compounds gave a predicted *in vivo* CL_{int} within two-fold of the derived *in vivo* CL_{int} and the AAFE for these predictions was 1.98, while for

non-regression corrected data as little as 16% fell within two-fold and the AAFE was 5.1 (Table 5).

Exploiting this IVIVE approach in animal models supporting projects

In Figure 4B, the prediction limits for a prospective *in vivo* CL_{int} value were used to define whether *in vitro* kinetic parameters for a new chemical series could be used to predict *in vivo* CL_{int}. The inner dashed lines represented the one-sided 90% upper and lower confidence limits for the regression line, based on variance

Table 5. Statistics for *in vivo* CL_{int} obtained after cross validation of the human and rat data set used for the regression lines compared with the non-regression corrected predictions. Within brackets are the results obtained when measured blood-to-plasma ratios ($n=30$) were substituted with estimated values.

	Human <i>in vivo</i> CL _{int} prediction	Non-regression corrected human CL _{int} prediction	Rat <i>in vivo</i> CL _{int} prediction	Non-regression corrected rat CL _{int} prediction
Within two-fold (%)	66 (68)	32 (37)	54	16
Within two- to five-fold (%)	29 (22)	24 (27)	45	30
>five-fold (%)	4 (10)	44 (37)	2	53
afe	1.00 (1.00)	3.8 (3.3)	0.98	4.8
aafe	1.90 (2.00)	4.2 (3.8)	1.98	5.1
Slope*	0.661 ± 0.002 (0.683 ± 0.02)	na	0.663 ± 0.042	na
Intercept*	0.633 ± 0.032 (0.601 ± 0.032)	na	0.974 ± 0.035	na

*Data is average ± SD of the six model groups of the cross validations (for further details see 'Methods'); na = not applicable.

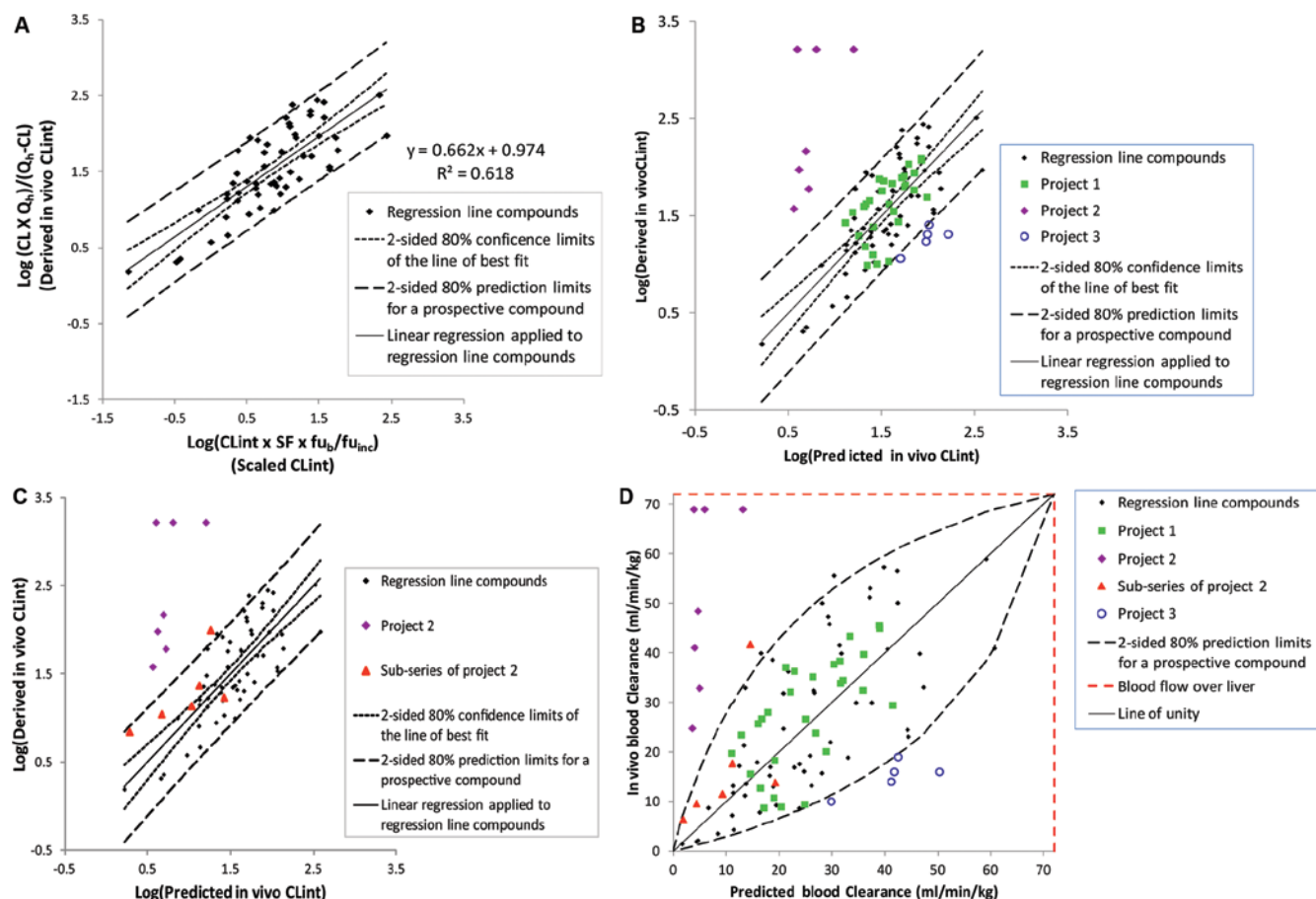


Figure 4. (A-D) The rat hepatocyte regression line (A), the corresponding regression corrected IVIVE plot with data from three AZ projects (B), data from AZ project 2 with additional data from a subsequent sub-series (C) and blood clearance data for regression reference compounds and AZ project compounds (D).

associated with the intercept and slope for the reference set. The outer prediction limits represent the variance for a future compound, accounting for the two components of variance; namely where the regression line can lie, and the variability (scatter) for a single compound about the regression line. Datasets from three AstraZeneca projects have been presented (Figure 4B). The compounds in project 1 lay within the outer prediction limits. The AFE and AAFE were calculated as 1.1 and 1.6, respectively, for the predicted *in vivo* CLint data and 75% of the compounds were predicted within two-fold of the derived *in vivo* CLint. For compounds from project 2, the derived *in vivo* CLint values were substantially under-predicted with all predicted *in vivo* CLint values outside the one-sided 90% upper limit. The AFE and AAFE for the CLint predictions were both equal to 52, and the derived *in vivo* CLint was >10-fold of the predicted values. In contrast, the predicted *in vivo* CLint values for compounds from project 3 were over-predicted with an AFE and AAFE of 0.2 and 5.2, respectively, and all compounds had predicted *in vivo* CLint values approximately five-fold above the derived *in vivo* CLint values.

Figure 4C demonstrated that following optimisation of project 2 chemistry, a subseries was obtained with improved IVIVE. The AFE and AAFE were 2.0 and 2.4, respectively.

In Figure 4D, the prediction limits associated with *in vivo* CLint have been converted to prediction limits for *in vivo* blood clearance (constrained by liver blood flow) Equation (10). The curved nature of the confidence interval illustrates why fold error in CLint prediction, rather than CL prediction, is a better measure of predictive power of the IVIVE method. The figure contains the data from all three projects, including the sub-series of project 2.

Discussion

During the development of new chemical entities within the pharmaceutical industry, the importance of being able to use *in vitro* data, in preference to costly and time consuming *in vivo* PK data, for efficient optimisation of compound properties, such as drug clearance, is well recognised. Therefore it is important that the accuracy of IVIVE is understood early on so that emphasis can be placed on *in vitro* data for design of low clearance compounds. It has previously been demonstrated that a regression offset approach can be applied to predict human *in vivo* CLint (Riley et al. 2005; Ito & Houston 2005; Grime & Riley 2006; Sohlenius-Sternbeck et al. 2010). This scaling approach adjusts for the systematic under-prediction observed when scaling *in vitro* raw CLint directly using physiological SFs and the unbound fractions. In short, a regression offset was established using *in vitro* and *in vivo* clearance data and the unbound fractions in blood ($f_{u,b}$) and the *in vitro* incubation ($f_{u,inc}$) from a set of reference compounds. The scaled CLint was then empirically corrected using this regression offset

equation. As previously described in the work by Riley et al. (2005), the relationship in Figures 3 and 4 is well explained by linearity.

To obtain a reliable regression line, it is important that the reference compounds that are used to build it are carefully selected. The most crucial characteristic of a compound included within the regression reference set is that its principal route of elimination is hepatic metabolism. If any renal clearance is known, this clearance value should be subtracted from the total clearance prior to derivation of the *in vivo* CLint. It is also important that a range of the most important drug-metabolising enzymes are covered. These and other additional key requirements are shown in Table 6. For compounds with a very high *in vivo* clearance, the derived *in vivo* CLint is highly sensitive to the *in vivo* blood clearance value used and the estimate of hepatic blood flow. A small change (or error) in the observed *in vivo* clearance has a large effect on the derived *in vivo* CLint value. This is an inherent consequence of the WSM. Thus, it is recommended that compounds with *in vivo* clearance approaching liver blood flow (within 10%) should not be included in the reference set defining the regression equation.

An advantage to the regression offset approach is that it provides the means to normalise CLint data generated over time that may vary due to changes in hepatocyte donor, *in vitro* incubation conditions or revision of physiological SF. This is managed through redefining the regression equation at appropriate junctures linked to implementation of any of the aforementioned changes. In a previous publication (Sohlenius-Sternbeck et al. 2010), a slightly different CLint assay set up was used and this resulted in somewhat different CLint values than reported here, which illustrates the importance of redefining the regression line. It is suggested that the robustness of the linear regression is monitored across time to ensure that any drift or significant changes to the *in vitro* assay outputs are discovered (e.g. a sub-set of the reference compounds could be assayed every 2 months or all reference compounds assayed every 6 months). This can be guided in part by the QC markers (also part of reference set) and the QC monitoring (Woodward & Goldsmith 1964), which is a formal statistical test to detect process level changes in an assay across time.

Table 6. Key requirements for compounds in a hepatocyte regression line.

Hepatic metabolism should be the principal route of elimination for the compounds.
In terms of metabolism, compounds in the reference set should cover a range of the most important drug-metabolising enzymes. Physical-chemistry and <i>in vitro</i> and <i>in vivo</i> parameters should cover a wide dynamic range.
Compounds with <i>in vivo</i> blood clearance values approaching liver blood flow (within 10%) should not be included.
Substrates known to undergo enterohepatic recirculation should not be included.
Substrates where cell permeability is dependent on hepatic uptake transporters should not be included.

Recent survey of the literature described high scarcity and variability of *in vitro* results obtained between laboratories (Nagilla et al. 2006). Therefore, any compound that is scaled, and empirically corrected, using the regression approach should be incubated under the same assay conditions described for the model reference set from which the regression line was generated. These considerations should also be taken into account and applied to the other *in vitro* parameters, such as the fractions unbound. It is noteworthy that providing a means to normalise CL_{int} data over time should prove valuable within projects for compound rank ordering and optimisation and also for generating predictive QSAR models, for properties, such as metabolic stability, from global datasets generated in different laboratories/assay formats.

A notable consequence of the regression approach is that the predicted *in vivo* CL_{int} is independent of the values taken for physiological SFs, such as hepatocellularity, liver and body weights. However, it is important to apply appropriate physiological SFs when the regression equation is defined so that a measure of the magnitude of unexplained under-prediction for the uncorrected scaling of CL_{int} is apparent from the regression intercept.

To the best of the authors' knowledge, an approach that can be used to set objective criteria for an acceptable IVIVE of CL_{int} that is linked to the quality of the kinetic data and integrity of the reference set is described for the first time. The empirically corrected extrapolations using the rat reference compounds can be used as a basis to assess the likelihood that rat *in vivo* clearance for a prospective compound or chemical series is predictable from *in vitro* kinetic data. It is proposed here that this can be achieved by setting an appropriate two-sided prediction interval on the regression corrected reference data. Any project compound or chemical series that lies within the pre-defined lower and upper prediction limits can be viewed as having an *in vivo* CL_{int} that was predictable based on its *in vitro* CL_{int} data. Conversely, if compounds tend to fall outside the recommended prediction interval, this infers an increased likelihood that the compound/series have derived *in vivo* CL_{int} values that are not well predicted by *in vitro* CL_{int} data.

This can be used to provide an objective view of risk within DMPK, where decisions are made relating to the most appropriate and efficient means to optimise compound design and ADME properties. The rat provides a useful model to validate the scaling approach, and given *in vivo* data can be generated to validate predictions from *in vitro* data as well as probe the mechanism of elimination. If the *in vitro* kinetics are predictive of *in vivo* clearance in rodents, there may be a reduced requirement for generating routine rodent pharmacokinetic studies as the basis for prioritising compounds for further testing. In this case, there is the opportunity to prioritise compound progression based on hepatocyte data in conjunction with *in vivo* pharmacodynamic (PD) data. Conversely, if the *in vivo* clearance is not

predictable, it may be prudent to use routine rodent pharmacokinetic studies to understand mechanism of clearance and/or establish an area where the *in vivo* kinetics can be more accurately predicted from *in vitro* data. If alternative elimination routes are identified, it should be determined if this elimination together with scaled hepatic clearance accounts for total clearance. The PK data can also be used in conjunction with additional *in vitro* data to elucidate other factors underlying the apparent IVIVE disconnect and assess whether these factors are likely to impact the IVIVE in man. For example, Soars et al. (2009) have previously shown how hepatocyte uptake experiments can be used to identify certain compounds that are outliers in a standard IVIVE approach and can be rationalised as substrates of hepatic transporters. Given the level of investment made in a compound by the time it reaches Phase 1 trials where human clearance can be estimated for the first time, primarily based on CL/F%, there is a great deal of emphasis placed on extrapolation of human *in vitro* CL_{int} data. If prediction of metabolic clearance cannot be established in pre-clinical species, it is challenging to rationalise how human kinetics can be predicted from *in vitro* data with any confidence.

In this work, it is shown that the regression offset approach can be used for identification of cases where the *in vitro* hepatic metabolic CL_{int} does not accurately predict the *in vivo* result. Predicted *in vivo* CL_{int} for a chemical series belonging to one AstraZeneca project (Project 3, Figure 4B) was found to be over-predicted. Subsequent experimental data suggested that compounds from this chemical series underwent hepatic glucuronidation followed by enterohepatic recirculation after hydrolysis by intestinal β -glucuronidases. In contrast to project 3, the IVIVE model was found to persistently under-predict compounds belonging to another AstraZeneca project (project 2, Figure 4B). Experimental data strongly suggested that the reason for the poor IVIVE in the rat was due to extensive biliary excretion of parent compound as a clearance pathway. However, after further optimisation of project chemistry the accuracy of IVIVE was improved (Figure 4C).

In summary, it is suggested that by establishing empirically corrected IVIVE, using appropriate reference compounds, the likelihood that the *in vivo* clearance is predictable from *in vitro* kinetic data for project compounds or chemical series can be estimated. This provides an objective means to identify compounds for progression in the project test cascade or to investigate further to optimise the chemistry into areas of chemical space where the *in vivo* clearance can be more accurately predicted from *in vitro* CL_{int} data. It is expected that future improvements to existing *in vitro* technologies, and understanding of mechanisms, will contribute to lessening the magnitude of systematic under predictions observed with IVIVE. Until such time, limitations with current scaling approaches can be dealt with by application of the regression correction to IVIVE.

Acknowledgements

The authors thank Annelie Bengtsson, Jessie Dahlström, Jenny Johansson, Olle Gissberg, Åse Husman Sjöblom, Ulrika Määttä and Ingemo Sjögren for laboratory support. All animal studies were approved by the Stockholm Södra Animal Research Ethical Board.

Declaration of interest

The authors report no conflicts of interest.

References

- Armitage P, Berry G. (1994). Statistical methods in medical research. Oxford: Blackwell Scientific Publications, 3rd edition.
- Barter ZE, Bayliss MK, Beaune PH, Boobis AR, Carlile DJ, Edwards RJ, Houston JB, Lake BG, Lipscomb JC, Pelkonen OR, Tucker GT, Rostami-Hodjegan A. (2007). Scaling factors for the extrapolation of *in vivo* metabolic drug clearance from *in vitro* data: reaching a consensus on values of human microsomal protein and hepatocellularity per gram of liver. *Curr Drug Metab* 8:33–45.
- Bissell DM, Guzelian PS. (1980). Phenotypic stability of adult rat hepatocytes in primary monolayer culture. *Ann N Y Acad Sci* 349:85–98.
- Brandon EF, Raap CD, Meijerman I, Beijnen JH, Schellens JH. (2003). An update on *in vitro* test methods in human hepatic drug biotransformation research: pros and cons. *Toxicol Appl Pharmacol* 189:233–246.
- Briem S, Martinsson S, Bueters T, Skoglund E. (2007). Combined approach for high-throughput preparation and analysis of plasma samples from exposure studies. *Rapid Commun Mass Spectrom* 21:1965–1972.
- Brown HS, Griffin M, Houston JB. (2007). Evaluation of cryopreserved human hepatocytes as an alternative *in vitro* system to microsomes for the prediction of metabolic clearance. *Drug Metab Dispos* 35:293–301.
- Brown RP, Delp MD, Lindstedt SL, Rhomberg LR, Beliles RP. (1997). Physiological parameter values for physiologically based pharmacokinetic models. *Toxicol Ind Health* 13:407–484.
- Delp MD, Evans MV, Duan C. (1998). Effects of aging on cardiac output, regional blood flow, and body composition in Fischer-344 rats. *J Appl Physiol* 85:1813–1822.
- Donato MT, Castell JV. (2003). Strategies and molecular probes to investigate the role of cytochrome P450 in drug metabolism: focus on *in vitro* studies. *Clin Pharmacokinet* 42:153–178.
- Floby E, Briem S, Terelius Y, Sohlenius-Sternbeck AK. (2004). Use of a cocktail of probe substrates for drug-metabolizing enzymes for the assessment of the metabolic capacity of hepatocyte preparations. *Xenobiotica* 34:949–959.
- Floby E, Johansson J, Hoogstraate J, Hewitt NJ, Hill J, Sohlenius-Sternbeck AK. (2009). Comparison of intrinsic metabolic clearance in fresh and cryopreserved human hepatocytes. *Xenobiotica* 39:656–662.
- Goodman LS, Limbird LE, Milinoff PB, Ruddon RW, Gilman AG. (1996). Goodman and Gilman's the pharmacological basis of therapeutics, 9th edition. New York: McGraw-Hill.
- Grime K, Riley RJ. (2006). The impact of *in vitro* binding on *in vitro*–*in vivo* extrapolations, projections of metabolic clearance and clinical drug-drug interactions. *Curr Drug Metab* 7:251–264.
- Hallifax D, Foster JA, Houston JB. (2010). Prediction of human metabolic clearance from *in vitro* systems: retrospective analysis and prospective view. *Pharm Res* 27:2150–2161.
- Hallifax D, Galetin A, Houston JB. (2008). Prediction of metabolic clearance using fresh human hepatocytes: comparison with cryopreserved hepatocytes and hepatic microsomes for five benzodiazepines. *Xenobiotica* 38:353–367.
- Hewitt NJ, Lechón MJ, Houston JB, Hallifax D, Brown HS, Maurel P, Kenna JG, Gustavsson L, Lohmann C, Skonberg C, Guillouzo A, Tuschl G, Li AP, LeCluyse E, Groothuis GM, Hengstler JG. (2007). Primary hepatocytes: current understanding of the regulation of metabolic enzymes and transporter proteins, and pharmaceutical practice for the use of hepatocytes in metabolism, enzyme induction, transporter, clearance, and hepatotoxicity studies. *Drug Metab Rev* 39:159–234.
- Houston JB. (1994). Utility of *in vitro* drug metabolism data in predicting *in vivo* metabolic clearance. *Biochem Pharmacol* 47:1469–1479.
- Houston JB, Carlile DJ. (1997). Prediction of hepatic clearance from microsomes, hepatocytes, and liver slices. *Drug Metab Rev* 29:891–922.
- Ito K, Houston JB. (2005). Prediction of human drug clearance from *in vitro* and preclinical data using physiologically based and empirical approaches. *Pharm Res* 22:103–112.
- Ito K, Houston JB. (2004). Comparison of the use of liver models for predicting drug clearance using *in vitro* kinetic data from hepatic microsomes and isolated hepatocytes. *Pharm Res* 21:785–792.
- Kilford PJ, Gertz M, Houston JB, Galetin A. (2008). Hepatocellular binding of drugs: correction for unbound fraction in hepatocyte incubations using microsomal binding or drug lipophilicity data. *Drug Metab Dispos* 36:1194–1197.
- Lave T, Dupin S, Schmitt C, Chou RC, Jaeck D, Coassolo P. (1997). Integration of *in vitro* data into allometric scaling to predict hepatic metabolic clearance in man: application to 10 extensively metabolized drugs. *J Pharm Sci* 86:584–590.
- Li AP, Lu C, Brent JA, Pham C, Fackett A, Ruegg CE, Silber PM. (1999). Cryopreserved human hepatocytes: characterization of drug-metabolizing enzyme activities and applications in higher throughput screening assays for hepatotoxicity, metabolic stability, and drug-drug interaction potential. *Chem Biol Interact* 121:17–35.
- Loi CM, Young M, Randinitis E, Vassos A, Koup JR. (1999). Clinical pharmacokinetics of troglitazone. *Clin Pharmacokinet* 37:91–104.
- McGinnity DE, Soars MG, Urbanowicz RA, Riley RJ. (2004). Evaluation of fresh and cryopreserved hepatocytes as *in vitro* drug metabolism tools for the prediction of metabolic clearance. *Drug Metab Dispos* 32:1247–1253.
- Nagilla R, Frank KA, Jolivet LJ, Ward KW. (2006). Investigation of the utility of published *in vitro* intrinsic clearance data for prediction of *in vivo* clearance. *J Pharmacol Toxicol Methods* 53:106–116.
- Naritomi Y, Terashita S, Kagayama A, Sugiyama Y. (2003). Utility of hepatocytes in predicting drug metabolism: comparison of hepatic intrinsic clearance in rats and humans *in vivo* and *in vitro*. *Drug Metab Dispos* 31:580–588.
- Obach RS. (1999). Prediction of human clearance of twenty-nine drugs from hepatic microsomal intrinsic clearance data: An examination of *in vitro* half-life approach and nonspecific binding to microsomes. *Drug Metab Dispos* 27:1350–1359.
- Obach RS, Lombardo F, Waters NJ. (2008). Trend analysis of a database of intravenous pharmacokinetic parameters in humans for 670 drug compounds. *Drug Metab Dispos* 36:1385–1405.
- Paine SW, Parker AJ, Gardiner P, Webborn PJ, Riley RJ. (2008). Prediction of the pharmacokinetics of atorvastatin, cerivastatin, and indomethacin using kinetic models applied to isolated rat hepatocytes. *Drug Metab Dispos* 36:1365–1374.
- Paixão P, Gouveia LF, Morais JA. (2009). Prediction of drug distribution within blood. *Eur J Pharm Sci* 36:544–554.
- Riley RJ, McGinnity DE, Austin RP. (2005). A unified model for predicting human hepatic, metabolic clearance from *in vitro* intrinsic clearance data in hepatocytes and microsomes. *Drug Metab Dispos* 33:1304–1311.
- Shibata Y, Takahashi H, Chiba M, Ishii Y. (2002). Prediction of hepatic clearance and availability by cryopreserved human hepatocytes: an application of serum incubation method. *Drug Metab Dispos* 30:892–896.

- Smith R, Jones RD, Ballard PG, Griffiths HH. (2008). Determination of microsome and hepatocyte scaling factors for *in vitro/in vivo* extrapolation in the rat and dog. *Xenobiotica* 38:1386-1398.
- Soars MG, Webborn PJ, Riley RJ. (2009). Impact of hepatic uptake transporters on pharmacokinetics and drug-drug interactions: use of assays and models for decision making in the pharmaceutical industry. *Mol Pharm* 6:1662-1677.
- Sohlenius-Sternbeck AK, Afzelius L, Prusis P, Neelissen J, Hoogstraate J, Johansson J, Floby E, Bengtsson A, Gissberg O, Sternbeck J, Petersson C. (2010). Evaluation of the human prediction of clearance from hepatocyte and microsome intrinsic clearance for 52 drug compounds. *Xenobiotica* 40:637-649.
- Stringer R, Nicklin PL, Houston JB. (2008). Reliability of human cryopreserved hepatocytes and liver microsomes as *in vitro* systems to predict metabolic clearance. *Xenobiotica* 38:1313-1329.
- Tang H, Hussain A, Leal M, Mayersohn M, Fluhler E. (2007). Interspecies prediction of human drug clearance based on scaling data from one or two animal species. *Drug Metab Dispos* 35:1886-1893.
- Wenlock MC, Potter T, Barton P, Austin RP. (2011). A method for measuring the lipophilicity of compounds in mixtures of 10. *J Biomol Screen* 16:348-355.
- Woodward RH and Goldsmith PL. (1964) Cumulative sum techniques. In: *Mathematical and statistical techniques for industry. Monographs*, 3. Edinburgh: Oliver and Boyd.
- Youdim KA, Zayed A, Dickins M, Phipps A, Griffiths M, Darekar A, Hyland R, Fahmi O, Hurst S, Plowchalk DR, Cook J, Guo F, Obach RS. (2008). Application of CYP3A4 *in vitro* data to predict clinical drug-drug interactions; predictions of compounds as objects of interaction. *Br J Clin Pharmacol* 65:680-692.